Meccanica (2011) 46:1363–1371
DOI 10.1007/s11012-010-9403-z

Emulation system for assessment of human-robot collision

B. Povse · D. Koritnik · R. Kamnik · T. Bajd · M. Munih

Received: 25 September 2009 / Accepted: 30 November 2010 / Published online: 10 December 2010

Abstract The research described is focused on cooperation of a small industrial robot and human operator where collision is expected only between the robot end-effector and the lower arm of the human worker. To study the effect of the impact between the robot and man, a passive mechanical lower arm (PMLA) was developed. The investigation presented in this paper evaluates whether the PMLA is a sufficiently accurate emulation system of a passive human lower arm. The same experiments were performed with the PMLA and with human volunteers. The results of both investigations were compared and evaluated in order to determine whether the PMLA can competently replace human volunteers in more dangerous investigations.

Keywords Physical human-robot interaction · Robot safety · Human-robot collision

B. Povse (✉) · D. Koritnik
R & D Department for Automation, Robotics and Electronic Instrumentation, Dax Electronic Systems Company, Vreskovo 68, Trbovlje, Slovenia
e-mail: borut.dax@siol.net

R. Kamnik · T. Bajd · M. Munih
Laboratory of Robotics and Biomedical Engineering, Faculty of Electrical Engineering, University of Ljubljana, Trzaska 25, Ljubljana, Slovenia

1 Introduction

In industry, optimization of production performance and introduction of new technologies require coexistence of humans and robots. Future robots will not work behind safety guards with locked doors or light barriers. Instead, they will be working in close cooperation with humans. This leads to a fundamental concern of how to ensure safe physical human-robot interaction.

Different approaches have been proposed to study human robot interaction safety [1–3]. However, human-robot collisions and resulting injuries were to our knowledge mainly investigated by the Institute of Robotics and Mechatronics, DLR—German Aerospace Center. Their studies included different industrial robots such as Kuka KR3-SI (weight 54 kg), Kuka KR6 (weight 235 kg), Kuka KR500 (weight 2350 kg) and a LWRIII (weight 14 kg) light-weight robot. The experiments were focused on chest and head impacts that can cause serious injury or even death. The estimation of injury was made using the head injury criteria and the compression or viscous criteria for the chest. The injury level was expressed using the abbreviated injury scale, classifying the injury severity from 0 (none) to 6 (fatal). The results of the dummy crash-tests indicated that no robot, whatever mass it has, could be life-threatening at the end-effector velocity of 2 m/s prior to impact when automobile industry criteria are used and clamping is excluded. Nevertheless, other less dangerous injuries such as fractures of

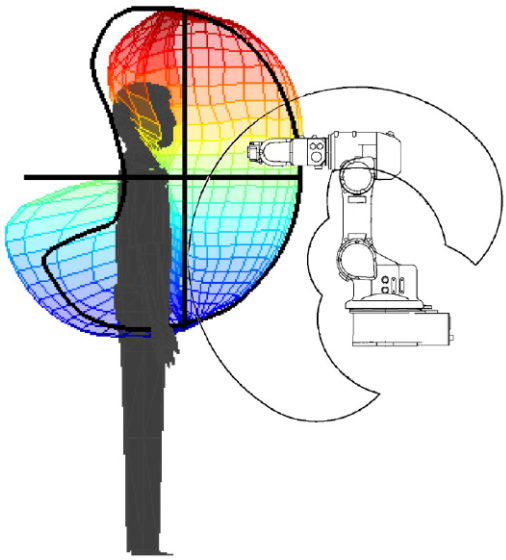

Fig. 1 Common human arm and robot workspace (side view)

facial and cranial bones can occur at typical robot velocities [4, 5]. When taking clamping of the human body in consideration both the head and chest can also be severely injured [6].

Our research is focused on cooperation of a small industrial robot manipulator and a human worker. Complex assembly is an example of an industrial cell where the robot and human can physically interact in order to make the assembly process more efficient and economical. Demanding operations (e.g. insertion of flexible parts) are performed by the human worker, while precise assembly of rigid parts is accomplished by a robot. We envisage an industrial cell with a common human-robot workspace as shown in Fig. 1 [7].

Another real-world example from our industrial experiences, where the worker and the robot could collaborate, is a wash machine assembly line. The assembly process comprises several phases. In two of these phases, the wiring and clamping is performed separately in two different assembly cells. In the first assembly cell, the worker wires the wash machine. In the second cell, the robot clamps the wires together. These two phases could be united into a single phase and also into a single assembly cell by unifying the human and robot workspace. While the worker wires the wash machine, the robot clamps together the wires already inserted. Therefore, the human-robot cooperation would save the place and shorten production cycle time. During the wiring, the worker's lower arms

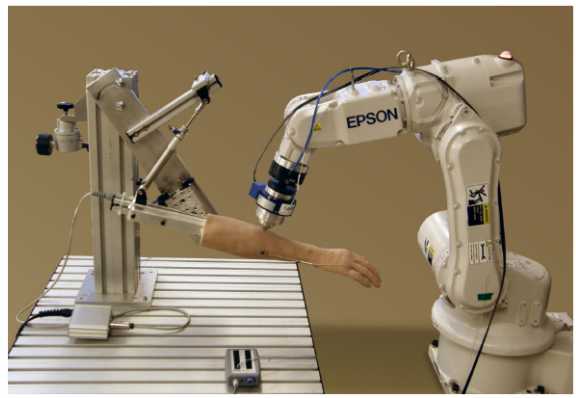

Fig. 2 PMLA and six-axis robot with point end-effector

are mostly in the same configuration as the mechanical lower arm shown in Fig. 2.

Collision is predominantly expected between the robot end-effector and the lower arm, wrist, or hand of the human operator. No life-threatening situations can occur; fractures of the lower arm bones are possible only in the worst-case scenario. The goal of our investigation is to answer the question of whether safe physical human robot interaction is possible when using a small standard industrial robot. To study the effect of the impact between the robot and man, a passive mechanical lower arm (PMLA) was developed and equipped with inertial sensors. The aim of the work described in this paper is to verify whether the PMLA is a sufficiently accurate emulation system of a passive human lower arm. To achieve this goal, the same experiments were performed with the PMLA and with human volunteers. The results of both investigations were compared and evaluated. The point of impact was chosen on the dorsal aspect of the lower arm where the bone is covered with thick muscle and adipose tissue. Collisions with bony prominences (e.g. wrist) were considered too dangerous for investigation with human volunteers.

To determine a safe range of experiments with human subjects, a preliminary investigation was performed with one of the authors of this paper. While incrementally increasing the robot end-effector deceleration up to 5 m/s^2 and the depth of the robot endpoint penetration into the arm skin and muscle tissue up to 30 mm, the test subject reported the pain intensity caused by each robot collision. The impacts with the plane end-effector at maximal end-effector velocity of 2 m/s did not cause any noticeable pain. Dur-

ing the experiments with the line end-effector tool, a mild pain intensity was rated by the test subject. We estimated the point impact experiments to be too dangerous for experiments with human volunteers. Only the safest plane and line impact experiments were performed. The results of the plane and line impact experiments with volunteers were then used to evaluate the behavior of the PMLA emulation system.

During the experiment, the volunteers had to determine the pain they felt after each impact on a scale from 0 (no pain) to 100 (unbearable pain). The pain was also used as a criterion to determine if the experiment could be continued with a particular subject. It was expected that the volunteers will only feel mild pain.

All volunteers gave their consent for participation in our investigation after detailed explanation of experimental procedures. We received the ethical approval for the investigation from the Slovenian medical ethics committee.

The results of all experiments were compared in order to determine whether the PMLA is a sufficiently accurate emulation system of a passive human lower arm and can validly replace human volunteers in future more dangerous investigations.

2 Methodology

2.1 Passive mechanical lower arm

A passive mechanical lower arm (PMLA) was built emulating relevant human arm characteristics. The device consists of a vertical base aluminum pillar to which the arm structure is attached (Fig. 2). The connection between the arm and the base is represented by a passively adjustable shoulder joint. Two smaller aluminum profiles, a pneumatic cylinder and a pneumatic rotary unit represent the PMLA structure. The aluminum profile connected to the vertical aluminum base pillar represents the upper arm. Its length is 280 mm. The pneumatic rotary unit connected to the aluminum upper arm represents the elbow joint and emulates the human biceps muscle. The working pressure of the rotary unit is 1.5–7 bar and it generates the torque of 5.5 N m at 5 bar. The torque produced by the rotary unit compensates for the gravity, similarly to the human biceps muscle, and holds the lower arm in a desired pose. The desired torque is set by adjusting the pressure regulating valve connected to the rotary unit. The viscoelastic properties of the human elbow are emulated using a pneumatic cylinder attached to the aluminum profiles representing the lower and upper arm. The length of the cylinder is 180 mm, its diameter is 16 mm and the maximal working pressure is 10 bar. The characteristic properties of the elbow joint (viscous damping and elasticity) can be determined by adjusting the airflow valves connected to the cylinder. The viscoelastic elbow joint properties [8] were determined by using a mathematical model of the human elbow ($B = 2$ N ms/rad, $K = 15$ N m/rad). The lower arm aluminum structure supports a foam rubber mock-up providing similar stiffness as relaxed muscle tissue [9]. The rubber mock-up is made from advanced prosthetic material (polyurethane foam). Length of the lower arm aluminum structure measured from the rotary unit rotation center to the wrist is 266 mm. The foam rubber mock-up is covered with a silicon esthetic glove resembling human skin. The weight of the mechanical lower arm is 2.10 kg. This value is in the range of the mean lower arm weight value for women (1.94 kg) and men (2.23 kg) according to [10].

2.2 Robot end-effectors

Industrial robots are equipped with different grippers and end-effectors according to the task they are performing. In order to take into consideration as many types of different impacts possible, the experiments with the PMLA included three generalized end-effectors for plane, line, and point impact (Fig. 3). The

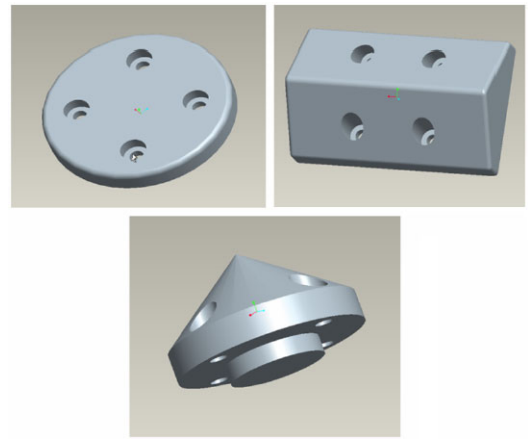

Fig. 3 Differently-shaped robot end-effectors for plane, line and point impact

experiments with human volunteers included only the plane and line end-effectors due to safety reasons. The point impact end-effector was considered to be too dangerous for human volunteer investigation. The line and the point impact end-effectors were approximated by the end-effectors with a slightly rounded edge or point.

2.3 Measuring system (PMLA investigation)

The measuring system used in the investigation comprised the inertial sensors incorporating a set of two three-axis accelerometers ADXL203 and three gyroscopes ADXRS150 (Analog Devices, Inc.), three axis force sensor (JR3, Inc.), and the optical measurement system Optotrak Certus (Northern Digital, Inc.). The inertial sensors were integrated into a single housing [11] and mounted to the lower arm aluminum bar extending to the opposite side of the mechanical elbow rotation center. The velocities and the accelerations were therefore measured at the PMLA-supporting aluminum bar and recalculated to the PMLA impact point at the surface of the lower arm. The force sensor was installed between the robot's sixth joint and the end-effector. The assessed accelerations, velocities and forces were logged during the human-robot collision by a real-time xPC target computer. In addition, the robot end-effector and PMLA were equipped with infrared markers as shown in Fig. 2. The first marker was placed onto the force sensor installed between the robot and the robot end-effector. The second marker was placed onto the right-side surface of the lower arm under the point of impact. The displacement of the robot end-effector and PMLA during the impact was assessed by the Optotrak position sensor that measured the motion of the infrared markers attached to robot and PMLA.

2.4 Measuring system (human volunteer investigation)

The experimental setup for the investigation with volunteers was almost identical to the setup used for the experiments with the PMLA. An important addition was a positioning device that helped to place the lower arm of the volunteer into the desired pose. The positioning device consisted of aluminum profiles and two wires (Fig. 4). With the help of these wires and the marks on the lower arm, the volunteer was able to place his arm into the same predefined starting pose.

Fig. 4 A human volunteer and the six-axis robot with the line end-effector

The second difference was the adapter used to attach the inertial sensor to the volunteer's lower arm. The adapter was composed of an aluminum supporting rod and two belts used to fasten the adapter with the inertial sensor to the lower arm.

2.5 Robot collision experiments

In our experiments, the robot end-effector collided with the PMLA or human lower arm perpendicularly at a constant deceleration. The point of impact was positioned midway between the wrist and the elbow on the dorsal aspect of the lower arm (Fig. 4). The robot end-effector was displaced toward the point of impact along a straight line. Several tests were carried out at maximal velocity, different robot decelerations, different depths of stop points with regard to the arm surface and different end-effectors. The maximal robot end-effector speed was 2000 mm/s. The robot end-effector deceleration was changed incrementally from 1000 mm/s^2 to 5000 mm/s^2. The end-effector stop point was located inside the lower arm. The depth from the lower arm surface was changed from 10 mm to 30 mm by 10 mm steps. After each robot impact, the PMLA or the human lower arm were placed into the predefined starting pose.

Fig. 5 Graphical user interface for pain intensity assessment

2.6 Pain intensity assessment

The human subjects had to determine the pain intensity they felt after each robot collision using a graphical user interface programmed in Visual Studio (Fig. 5). They were asked to rate the pain intensity by moving the slider to the value that best described the pain intensity felt during collision with the robot. A linear pain intensity scale was drawn along the slider, ranging from 0 (no pain- left slider position) to 100 (unbearable pain-right slider position) [12]. The scale [13] was divided into following five areas:

- 0 . . . 20 No pain,
- 20 . . . 40 Mild pain,
- 40 . . . 60 Moderate pain,
- 60 . . . 80 Horrible pain,
- 80 . . . 100 Unbearable pain.

To ensure valid pain assessment, the experiments were performed in a randomized order. The results were compared and correlated with the impact energy density values. Namely, higher impact energy density is expected to cause higher pain intensity. The impact energy density was defined as

$$e_A = \frac{\int_{s_{\text{impact\_start}}}^{s_{\text{impact\_stop}}} F \cdot ds}{A_{\text{end-effector}}}. \tag{1}$$

In (1), F is the impact force applied to the lower arm; $s_{\text{impact\_start}}$ and $s_{\text{impact\_stop}}$ are the distances between the robot end-effector and the center of the lower arm at the start and at the end of the impact, while $A_{\text{end-effector}}$ is the contact surface area between the robot end-effector and the lower arm surface. The impact force F was measured using the JR3 force sensor. The interval of integration $[s_{\text{impact\_start}}, s_{\text{impact\_stop}}]$ was determined using Optotrak position measurements of the infrared markers attached to the lower arm and the robot end-effector. The effective contact surface area used in the calculations was measured using a stamp method. The end-effector was dipped into ink and pressed onto the lower arm. Afterwards, the imprint surface was measured. During the impact the robot end-effector's kinetic energy is transferred to the lower arm tissue (foam for the PMLA) only from the point where the end-effector touches the lower arm ($s_{\text{impact\_start}}$) to the point where the distance between the end-effector and the lower arm center is the smallest ($s_{\text{impact\_stop}}$). After that point, the robot end-effector kinetic energy is transferred to the lower arm kinetic energy, since the robot end-effector starts to push the lower arm. The energy received by the tissue divided by the contact surface area is the impact energy density (1) [14].

3 Results

3.1 Robot impact investigation results

In experiments the robot end-effector started at the maximum speed perpendicularly towards the PMLA while the robot end-effector deceleration (acceleration) and the stop point depth were changed respectively. At robot deceleration set to 1000 mm/s^2 three experiments were carried out with the robot end-effector stop point selected from 10 mm to 30 mm (by 10 mm steps) inside the PMLA. For each robot deceleration increment of 1000 mm/s^2, all three experiments were repeated. Altogether fifteen different measurements were performed for each robot end-effector. The impact force, PMLA speed, and PMLA acceleration were logged at 8 kHz by the real-time xPC target computer.

The measuring results sampled at high frequency provide us with adequate insight into the impact of the robot end-effector and the lower arm. The impact forces at constant deceleration and various end-effector stop point depths are shown in Fig. 6. The highest impact force was assessed about 30 ms after the start of impact and was highly dependent upon the robot end-effector stop point depth. The speed of the impact point was measured using the three-axis gyroscope and is shown in Fig. 7. The corresponding accelerations of the impact point are shown in Fig. 8.

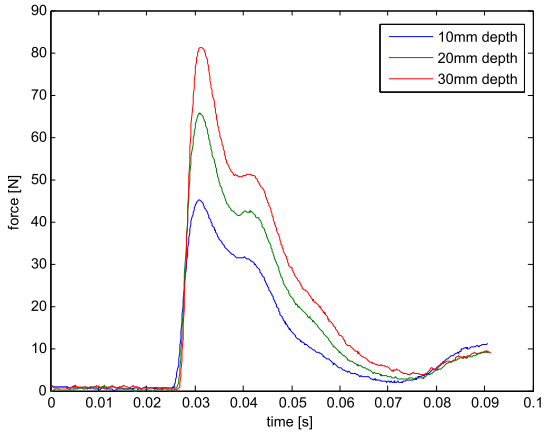

Fig. 6 The contact force during impact, PMLA investigation (robot acceleration 5000 mm/s^2, plane end-effector) at different depths of the stop point

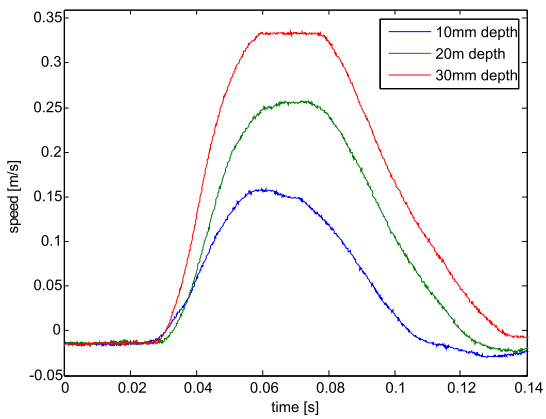

Fig. 7 The speed of the impact point, PMLA investigation (robot acceleration 5000 mm/s^2, plane impact end-effector)

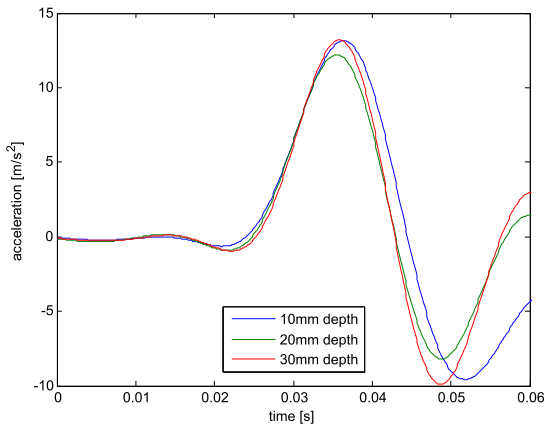

Fig. 8 The acceleration of the impact point, PMLA investigation (robot acceleration 5000 mm/s^2, plane impact end-effector)

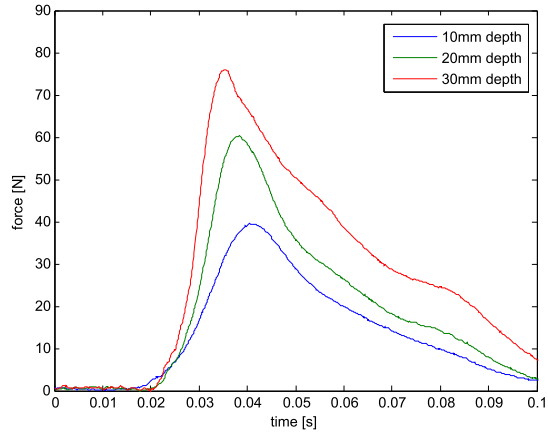

Fig. 9 The contact force during impact, human volunteer investigation (robot acceleration 5000 mm/s^2, plane end-effector) at different depths of the stop point

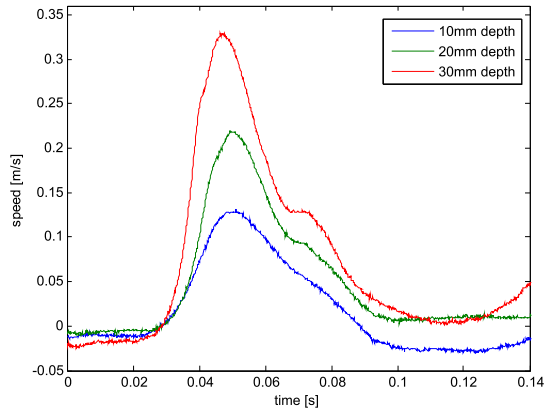

Fig. 10 The speed of the impact point, human volunteer investigation (robot acceleration 5000 mm/s^2, plane impact end-effector)

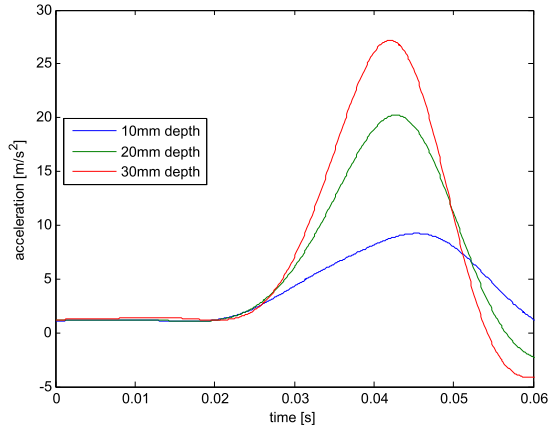

Fig. 11 The acceleration of the impact point, human volunteer investigation (robot acceleration 5000 mm/s^2, robot speed 2000 mm/s, plane impact end-effector)

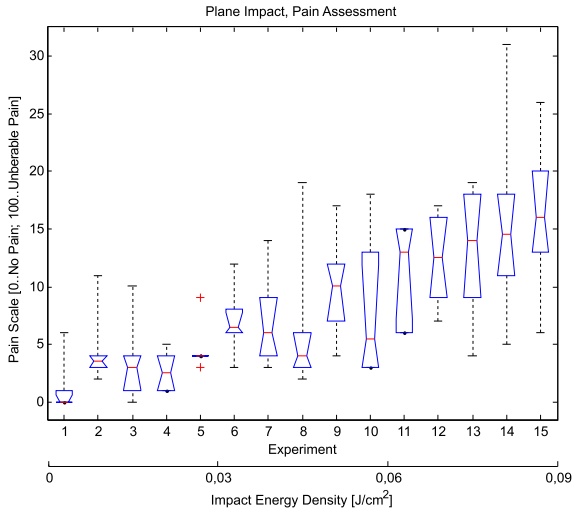

Fig. 12 Volunteer pain assessments, plane impact end-effector

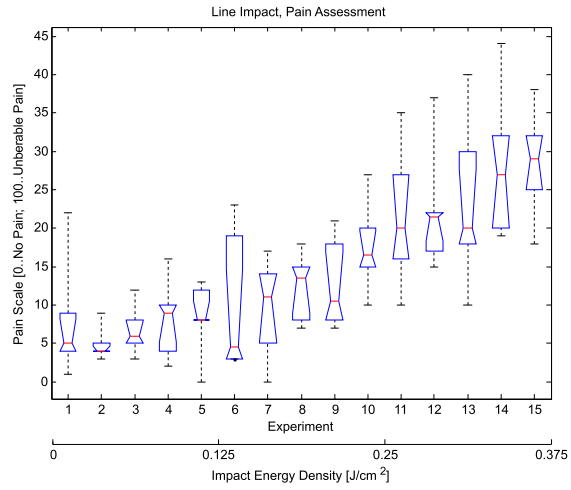

Fig. 13 Volunteer pain assessments, line impact end-effector

The same experiments as with the PMLA were repeated with six human volunteers. The results assessed in one of the subjects while using the plane end-effector are displayed in Figs. 9, 10, 11.

When comparing experiments with the PMLA and the human volunteers, the contact force had the same maximal values in both cases, but the shape of the curves was slightly different as shown in Fig. 6 and Fig. 9. The impact point speed also had similar maximal values with slightly different shape of the curves in both experiments (Fig. 7 and Fig. 10). The biggest difference between experiments was in the acceleration of the impact point, as can be observed from Fig. 8 and Fig. 11.

3.2 Pain assessment

The results of the pain assessment are shown in Figs. 12 and 13 using boxplot presentations in terms of median values (bold solid lines), 25th and 75th percentile values (error boxes), and 5th and 95th percentile values (error bars).

The upper horizontal axis shows the collision experiments ordered according to the ascending impact energy density. The lower horizontal axis divides the experiments into three groups according to the assessed impact energy density values. For example in experiments from one to five (Fig. 13), the assessed impact energy densities are within the range of 0 to 0.125 J/cm^2. The vertical axis represents the pain intensity on a scale from 0 to 100. For both plane and line impact experiments, the Spearman correlation factor was calculated, to evaluate the correlation between pain assessment and impact energy density. The plane impact results have $p = 0.002$ and $\rho = 0.31$ while the line impact experiment results have $p < 0.001$ and $\rho = 0.67$.

4 Discussion

The PMLA proved to be a good emulation system of a passive human lower arm during robot impact. In both human subjects and PMLA experiments the impact force and the impact point speed had similar maximal values with slightly different shapes of the curves. The impact point acceleration, however, had a different maximal value as well as different shape. The PMLA can, therefore, validly replace human volunteers when only impact force or impact point speed are considered and evaluated.

The highest pain intensity assessed by the human volunteers was in the mild pain area, as was expected from the preliminary experiments with one of the authors of this paper. The pain intensity assessments show high correlation with the impact energy density. However, the line impact assessments show a stronger correlation with the impact energy densities than the plane impact assessments, since the line end-effector collisions generate higher impact energy densities resulting in a wider and more reliable range of assessed pain intensities. The assessments of pain in-

tensity also represent useful data for physical human-robot interaction planning in terms of allowable robot end-effector speed and contact force. When human worker and industrial robot cooperate in the same workspace even minor contusions or wounds cannot be permitted. We, therefore, assume that low pain can be considered as an appropriate criterion for the selection of the permissible robot movements while cooperating with human. The pain threshold should not overcome the mild pain region during human-robot physical interaction.

In our experiments the robot end-effector collided with the PMLA or human lower arm perpendicularly at a constant deceleration. These were considered to be "safe" experiments which can be carried out with human volunteers. In literature the tolerance values were published regarding the energy density of the impact and the corresponding injury. Tissue injuries occur at an impact energy density higher than 2.52 J/cm^2, while hematoma or suffusions occur already below this value [15]. In our investigation the plane and line impact energy density values were considerably below 2.52 J/cm^2 [16]. In our further investigations more dangerous experiments will be performed only with the PMLA. The robot end-effector will be displaced toward the point of impact along a straight line at a constant speed or constant acceleration. Clamping of the human body is also possible in human-robot cooperation and can lead to severe injuries [6]. Experiments with clamping of the arm will not include human volunteers but will be carried out with the PMLA and modified measuring system incorporating higher impact force capabilities.

Before execution of further experiments, the mechanical properties of the PMLA will be altered in such a way that the differences between PMLA and human responses to robot impact will be decreased. The most advanced available prosthetic material was used to build the present lower arm of the PMLA. However, the results imply that the prosthetic material selected is not an adequate representation of the human lower arm soft tissue during impact. A new mechanical lower arm will be built using one, two, or even three layers of different materials representing relaxed muscle, adipose tissue, and skin. Further elasticity analyses including compressive and tensile stress measurements will be carried out in order to select the most suitable materials for human arm soft tissue representation. The robot will press the end-effector into different test samples and also into the human lower arm soft tissue to the predefined depth. The experiment will be repeated with different end-effectors at different velocities. The most suitable materials will be chosen by comparing human muscle tissue and different samples measurement data.

It is crucial for our further investigations to achieve a high level of similarity between human volunteer measurements data and PMLA impact responses. This is of great importance since the main criterion providing estimates of potential physical trauma and pain felt by a human in PMLA experiments is based on the impact force and impact energy density [15, 17] which highly depend on the biomechanical properties of soft tissue.

Acknowledgements This work was supported in part by the European Union. "Operation part financed by the European Union, European Social Fund."

References

1. Ikuta K, Ishii H, Nokata M (2003) Safety evaluation method of design and control for human-care robots. Int J Robot Res 22(5):281–298
2. Heinzmann J, Zelinsky A (2003) Quantitative safety guarantees for physical human-robot interaction. Int J Robot Res 22(7–8):479–504
3. Lim H-O, Tanie K (2000) Human safety mechanisms of human-friendly robots: passive viscoelastic trunk and passively movable base. Int J Robot Res 19(4):307–335
4. Haddadin S, Albu-Schäffer A, Hirzinger G (2007) Safety evaluation of physical human-robot interaction via crash-testing. In: Robotics: science and systems conference (RSS2007), Atlanta, USA
5. Haddadin S, Albu-Schäffer A, Hirzinger G (2008) The role of the robot mass and velocity in physical human-robot interaction—part I: unconstrained blunt impacts. In: IEEE international conference on robotics and automation (ICRA2008), Pasadena, USA, pp 1331–1338
6. Haddadin S, Albu-Schäffer A, Hirzinger G (2008) The role of the robot mass and velocity in physical human-robot interaction—part II: constrained blunt impacts. In: IEEE international conference on robotics and automation (ICRA2008), Pasadena, USA, pp 1339–1345
7. Klopcar N, Tomsic M, Lenarcic J (2007) A kinematic model of shoulder complex to evaluate the arm-reachable workspace. J Biomech 40:86–91
8. Kodek T, Munih M (2003) An analysis of static and dynamic joint torques in elbow flexion-extension movements. Simul Model Pract Theory 11:297–311
9. Federico S, Grillo A, Giaquinta G, Herzog W (2009) A semi-analytical solution for the confined compression of hydrated soft tissue. Meccanica 44(2):197–205
10. de Leva P (1996) Adjustments to Zatsiorsky-Seluyanov's segment inertia parameters. J Biomech 29(9):1223–1230

11. Music J, Kamnik R, Munih M (2006) Model based inertial sensing of human body motion kinematics in sit-to-stand movement. Simul Model Pract Theory 16:933–944
12. Katz J, Melzack R (1999) Measurement of pain. Surg Clin North Am 79:231–252
13. Collins SL, Moore RA, McQuay HJ (1997) The visual analogue pain intensity scale: what is moderate pain in millimeters? Pain 72:95–97
14. Povse B, Koritnik D, Maver T, Kamnik R, Bajd T, Munih M (2009) Cooperation of small industrial robot and human operator. In: 18th international workshop on robotics in Alpe-Adria-Danube region (RAAD 2009), Brasov, Romania, pp 1339–1349
15. Haddadin S, Albu-Schäffer A, Hirzinger G (2007) Safe physical human-robot interaction: measurements, analysis & new insights. In: International symposium on robotics research (ISRR2007), Hiroshima, Japan
16. Haddadin S, Albu-Schäffer A, De Luca A, Hirzinger G (2008) Evaluation of collision detection and reaction for a human-friendly robot on biological tissues. In: IARP international workshop on technical challenges and dependable robots in human environments, Pasadena, USA
17. Yamada Y, Hirasawa Y, Huand S, Umetani Y, Suita K (1997) Human-robot contact in the safeguarding space. IEEE/ASME Trans Mechatron 2(4):230–236